Boosting System Options for High Efficiency Fuel Cell Electric Vehicles

A. Kerviel [1,2], A. Pesyridis [1] and D. Chalet [2]

[1] Department of Mechanical, Aerospace and Civil Engineering, Brunel University, London, UK
[2] Ecole Centrale de Nantes, LHEEA lab. (ECN/CNRS), Nantes, FRANCE

Abstract:

Mass-produced, off-the-shelf automotive air compressors cannot be directly used for boosting a fuel cell vehicle (FCV) application in the same way they are used in internal combustion engines, since requirements are different: a high pressure ratio with a low mass flow rate combined with a high efficiency requirement and compact size. From the established fuel cell types, the most promising for application in passenger cars or light commercial vehicle applications is the proton exchange membrane fuel cell (PEMFC), operating at around 80°C. In this case, an electric assisted turbocharger (E-turbocharger) and electric supercharger (single or two-stage) are more suitable than screw and scroll compressors. In order to determine which type of these boosting options is the most suitable for fuel cell vehicle (FCV) application and to assess their individual merits, a co-simulation between GT-SUITE and MATLAB/SIMULINK of FCV powertrains is realised to compare vehicles performances on the Worldwide Harmonised Light Vehicle Test Procedure (WLTP) driving cycle. Results show that the vehicle equipped with an E-turbocharger has higher performances than vehicle equipped with a two-stage compressor in the aspects of electric system efficiency (+1.6%) and driving range (+3.7%) but, for the same maximal output power, the vehicle's stack is 12.5% heavier and larger. Then, thanks to the turbine, the E-turbocharger leads to higher performances than the single stage compressor for the same stack size.

Key words: Boosting option, E-turbocharger, Fuel cell vehicle, PEMFC

Nomenclature

$Coeff_{pressure}$	Pressure loss coefficient	$P_{A,out}$	Outlet air pressure
$Dm_{A,in}$	Inlet air mass flow	P_{comp}	Compressor required power
$Dm_{A,out}$	Outlet air mass flow	$P_{H,in}$	Inlet hydrogen pressure
Dm_{eject}	Ejected air mass flow	P_{H2}	Average hydrogen pressure
$Dm_{H,in}$	Inlet hydrogen mass flow	P_{O2}	Average oxygen pressure
$Dm_{H,out}$	Outlet hydrogen mass flow	P_{sat}	Water saturation pressure
$Dm_{O,in}$	Inlet oxygen mass flow	R	Gas constant
$Dm_{O,out}$	Outlet oxygen mass flow	R_{eff}	Stack electric efficiency
E_{Nerst}	Nerst potential	$R_{eff,system}$	System efficiency
F	Faraday constant	R_i	Internal cell resistance
I	Current	T	Operating temperature
i	Current density	V_{act}	Activation losses
i_L	Limiting current density	V_{cell}	Cell voltage
N	Number of cells	V_{conc}	Mass transfer losses
P	Stack output power	V_{ohm}	Ohmic losses
$P_{A,in}$	Inlet air pressure		

1-Introduction

An Intergovernmental Panel on Climate Change (IPCC) study [1] from 2014 showed that 14% of global greenhouse gas emissions are due to transportation. Since 65% of greenhouse gas emissions are CO_2, it has become crucial to decrease their global warming impact. Taking well-to-wheel emissions into consideration, electric vehicles reach 180 g CO_2 eq/km (because of a global 68% oil, gas and coal electricity production) whereas fuel cell vehicles (FCVs) reach 127 g CO_2 eq/km [2][3]. Even if current regulations only take into account tank-to-wheel emissions, which are null for both of these types of vehicle, some car manufacturers such as Toyota (Mirai), Honda (Clarity Fuel Cell) or Daimler Group (GLC F-cell) are investing in fuel cell technology to prepare an uncertain future. To become a viable solution for transportation, fuel cell vehicles must deal with power density challenge. For instance, the Hyundai Tucson Fuel Cell edition is 300 kg heavier than the gasoline version for the same output power. To decrease the weight of the fuel cell vehicle means less fuel consumption and so higher driving range.

There is a large potential for increasing power density by using boosting system for the air supply. A higher pressure of the air means a higher output power and efficiency. A recent paper from Honda underlines that increase the pressure ratio from 1.0 to 1.7 provided 10% more output power [4]. As a consequence, it is possible to reduce the number of cells and so the weight of the fuel cell stack for the same output power. Given that the requirements differ from internal combustion engine (ICE), the choice of compressor type must be adapted to fuel cell vehicle application.

In order to determine which type of compressor to use, a literature review has been done to identify which types of fuel cell are relevant to transportation application. Then, fuel cell vehicle powertrain models have been developed, using a co-simulation between GT-SUITE and MATLAB/SIMULINK. Finally, simulations have been made on driving cycle to analyse the impact of the air supply system on vehicle performances.

2-Types of fuel cell

Fuel cells can be used in a large range of applications, including cars, trucks and power-stations. Then, fuel cell has a higher efficiency than ICE since it is a classical electrochemical cell which is not limited by the efficiency of Carnot cycle as thermal machines are.

They are firstly classified according to the type of electrolyte they employ. It determines the type of catalysis necessary, the operating temperature and reactions into the cell such as steam reforming. Finally, fuel cells are classified in function of the temperature at which the stack operates.

As seen in table 1, high operating temperature fuel cell does not require expensive catalysis such as platinum and allows steam reforming (internal transformation of light fuels into hydrogen). The major issue with this type of cell is that quick-starts are not allowed which makes transportation application almost impossible. To solve this problem, electric resistances can be used but it is a huge waste of energy. For instance, 4 Wh are necessary for a 200 W SOFCs stack to warm-up from 20°C to 700°C in 5 minutes [7]. Nissan managed to build the first SOFCs vehicle in 2016, using a 5 kW stack as an extender for the 24 kWh battery [8].

Low operating temperature fuel cells allow quick start but not steam reforming which limits usable fuel type. Thanks to high power density with a low operating temperature condition, a lower environmental impact than PAFCs and a non-sensitivity to CO_2 present in the air, PEMFC is the most suitable fuel cell type for a transportation application. It includes personal and mass transit vehicle. As an example, Toyota sells the Sora which is a fuel cell bus using two 114 kW PEMFCs stack from the personal fuel cell Toyota vehicle named Mirai [9].

Table 1: Fuel cell type classification [5] [6]

High operating temperature fuel cell	**Name of fuel cell**	**Solid oxide fuel cell (SOFC)**	**Molten carbonate fuel cell (MCFC)**
	Electrolyte	Hard, non-porous ceramic	Molten carbonate salt mixture
	Operating Temperature	600 – 1100 °C	650°C
	Fuel	Pure hydrogen, biogas or light fossil fuel	Hydrocarbon fuels
	Benefits	• Non-precious metal for catalysis • Able to reform methanol and ethanol	• Non-precious metal for catalysis • Efficiency : from 50% to 85% with cogeneration • No carbon monoxide or dioxide poisoning
	Drawbacks	• High operating temperature • Complexity of heat management	• High operating temperature • Poisoning by sulphur • Use hydrocarbon fuel = greenhouse gas emissions

Low operating temperature fuel cell	**Name of fuel cell**	**Proton exchange membrane fuel cell (PEMFC)**	**Alkaline fuel cells (AFCs)**	**Phosphoric acid fuel cell (PAFCs)**
	Electrolyte	Solid polymer (acid membrane)	Polymer (alkaline membrane)	Liquid phosphoric acid
	Operating Temperature	80 – 100 °C	100 – 250°C	250 – 300 °C
	Fuel	Pure hydrogen or methanol/ethanol (direct or indirect)	Pure hydrogen, borohydride or zinc	Hydrocarbon fuel
	Benefits	• Low operating temperature • Quick start • Environmentally friendly • High power density	• High efficiency (60%) • Non precious metal for catalysis	• High power (over 75 MW) • High overall efficiency (80%) when combined with cogeneration
	Drawbacks	• Use platinum for the catalysis • Sensitive to carbon monoxide • Water management	• Sensitive to carbon dioxide (the percentage in the air is enough to destroy the cell)	• Greenhouse gas emissions • Low efficiency without cogeneration (less than 40%)

When PEMFCs are supplied with ethanol or methanol, the chemical reaction releases CO_2 as follows [10]:

$$C_2H_5OH + 3O_2 = 2CO_2 + 3H_2O \qquad (1)$$

Pure hydrogen PEMFCs are more suitable than direct ethanol or methanol PEMFCs to comply with standards regarding CO_2 emissions since the chemical reaction only releases water as follows:

$$\frac{1}{2}O_2 + H_2 = H_2O \quad (2)$$

3- Boosting systems for Fuel Cells

As ICEs use air compressors to increase the power density and the efficiency of the engine, a boosting system can be used with a fuel cell stack to increase performances. However, the requirements are not the same. First, it needs a high pressure with a low air mass flow rate. Second, because of the battery, the stack, the control power unit and the hydrogen storage tanks, the size of the boosting system is significant in a transportation application. In most ICE applications, a turbocharger is used to recover the energy from high temperature burning gas. Even if an expander is used, the operating temperature of the PEMFC (80°C) is too low to recover enough power to drive the compressor. It implies that the air supply system uses power from the stack. As a consequence, a high efficiency is there an important requirement.

Table 2: comparison of centrifugal, roots, screw and scroll compressor [11] [12] [13] [14] [15]
*: very bad
**: bad
***: good
****: very good
*****: excellent

Type of compressors	 **Centrifugal**	 **Roots**	 **Screw**	 **Scroll**
Compactness	★ ★ ★ ★ ★	★ ★ ★	★	★
Weight	★ ★ ★ ★	★ ★ ★	★ ★	★ ★
Temperature rise	★ ★ ★	★	★ ★ ★ ★	★ ★ ★
Pulsations, noise	★ ★ ★ ★	★ ★	★ ★ ★	★ ★ ★
Compression	★ ★ ★	★ ★ ★	★ ★ ★ ★	★ ★ ★ ★
Cost	★ ★ ★ ★	★ ★ ★ ★ ★	★ ★	★ ★
Durability	★ ★ ★	★ ★ ★ ★	★ ★ ★	★ ★ ★
Average rating	**3.7/5**	**3.0/5**	**2.7/5**	**2.6/5**

As seen in table 2, centrifugal and roots compressors are the most suitable for a fuel cell application. Smaller and cheaper than screw and scroll compressors, they help to reduce the weight and the cost of PEMFCs vehicle which is already increased by the use of platinum.

Daimler, General Motor and SAIC changed their boosting option to centrifugal compressor (E-turbocharger) [11]. The Honda FCX Clarity used a screw compressor but the new Honda Clarity Fuel Cell is now equipped with a two-stage centrifugal compressor which has a 50% smaller sound absorber than the FCX screw compressor [4]. Toyota remains the only FCV manufacturer to use a root compressor (6 lobes). This type of compressor has lower efficiency and pressure ratio but higher power density than centrifugal one. However, the pulsation noise implies the use of bigger sound absorber. As a result, centrifugal compressors have been adopted by FCV manufacturers as the most suitable compressor type for fuel cell application.

Two-stage compressor and E-turbochargers are currently use for FCV application. The Honda Clarity Fuel Cell two-stage compressor reaches a 4:1 pressure ratio [4]. An estimated value of 2.8:1 pressure ratio is given by a recent paper for E-turbocharger [16]. This paper also proposed a mixed architecture with a two-stage compressor and a turbine-generator to reduce the energy consumption of the boosting system.

4- Models of fuel cell vehicle powertrain

Polarization curve model has been used to model the operation of a mono-cell pure hydrogen PEMFC with MATLAB/SIMULINK. The model, proposed by Pukrushpan [17], used in the MATLAB/SIMULINK environment is described by the following equations:

$$V_{cell} = E_{nerst} - V_{act} - V_{conc} - V_{ohm} \tag{3}$$

$$E_{nerst} = 1.229 - 0.85 * 10^{-3}(T - 298.15) + \frac{RT}{2F}\log(P_{H2} * P_{O2}^{0.5}) \tag{4}$$

$$V_{act} = v_0 + v_a[1 - \exp(-c_1 * i)] \tag{5}$$

$$V_0 = 0.279 - 0.85 * 10^{-3}(T - 298.15) + \frac{RT}{2F}\log[\,(P_{H,in} - P_{sat}) * 0.1173 * (P_{A,in} - P_{sat})^{0.5}] \quad (6)$$

$$V_a = [-1.618 * 10^{-5} * T + 1.168 * 10^{-2}]\left[\frac{P_{O2}}{0.1173} + P_{sat}\right]^2 + [1.8 * 10^{-4} * T - 0.166]\left[\frac{P_{O2}}{0.1173} + P_{sat}\right] + [-5.8 * 10^{-4} * T + 0.5736] \quad (7)$$

$$V_{conc} = i * \left(c_2 * \frac{i}{i_L}\right)^{c_3} \quad (8)$$

$$c_2 = [8.66 * 10^{-5} * T - 0.068)\left[\frac{P_{O2}}{0.1173} + P_{sat}\right] - (1.6 * 10^{-4} * T + 0.54) \quad (9)$$

$$V_{ohm} = R_i * i \quad (10)$$

Where V_{cell} is the output tension of the mono-cell. E_{nerst} is the Nerst potential. V_{act}, V_{conc} and V_{ohm} are respectively the activation, mass transfer and ohmic losses. C_1 and C_3 are given by a recent paper concerning air supply system control [18] as $C_1 = 10$ and $C_3 = 2$.

The total output power of the N-cells stack is calculated as:

$$P = N * V_{cell} * I \quad (11)$$

The electrochemical reaction is considered as stoichiometric. The system is supposed to run with an excess of air. The current is calculated from the hydrogen mass flow rate and the excess of air is included in the calculation of oxygen partial pressure. As a result, P_{O2} and P_{H2} from previous equations are calculated by taking the average between the inlet and outlet stack pressure as follows:

$$P_{O2} = 0.5 * (P_{A,in} * 0.21) * (1 + \frac{Dm_{O,out}}{Dm_{O,in}}) \quad (12)$$

$$P_{H2} = 0.5 * P_{H,in} * (1 + \frac{Dm_{H,out}}{Dm_{H,in}}) \quad (13)$$

Where $Dm_{O,in}$ and $Dm_{H,in}$ are the inlet mass flow rates and $Dm_{O,out}$ and $Dm_{H,out}$ are the outlet mass flow rates of oxygen and hydrogen, respectively. $P_{A,in}$ and $P_{H,in}$ are the inlet pressures of air and hydrogen.

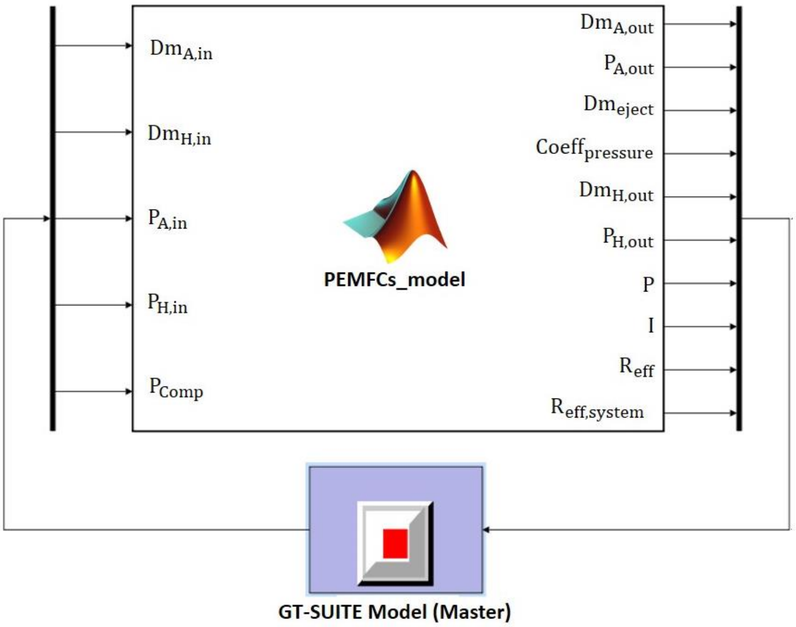

Fig.1: MATLAB/SIMULINK diagram using a Matlab function (PEMFCs_model) and a GT-SUITE master block

As seen in Fig. 1, the MATLAB/SIMULINK model runs as a black box in GT-SUITE environment. The "PEMFC_model" refers to the MATLAB function using the model described. The inputs are the inlet mass flow rates ($Dm_{A,in}$, $Dm_{H,in}$), the inlet pressures ($P_{A,in}$, $P_{H,in}$) and the required power by air supply system (P_{comp}). The outputs include the outlet mass flow rates ($Dm_{A,out}$, $Dm_{H,out}$), the outlet air pressure ($P_{A,out}$), the output produced power, the current and the electric efficiencies (P , I , R_{eff} , $R_{eff,system}$). There are different ways of calculating the electric efficiency. In this paper, it is the electric stack efficiency and the electric system efficiency which are considered and calculated as follow [4] [19] [20]:

$$R_{eff} = \frac{P}{1.481 * N * I} \tag{12}$$

$$R_{eff,system} = \frac{P - P_{comp}}{1.481 * N * I} \quad (13)$$

Where N is the number of cells and 1.481 is the theoretical voltage at the terminals of a hydrogen fuel cell.

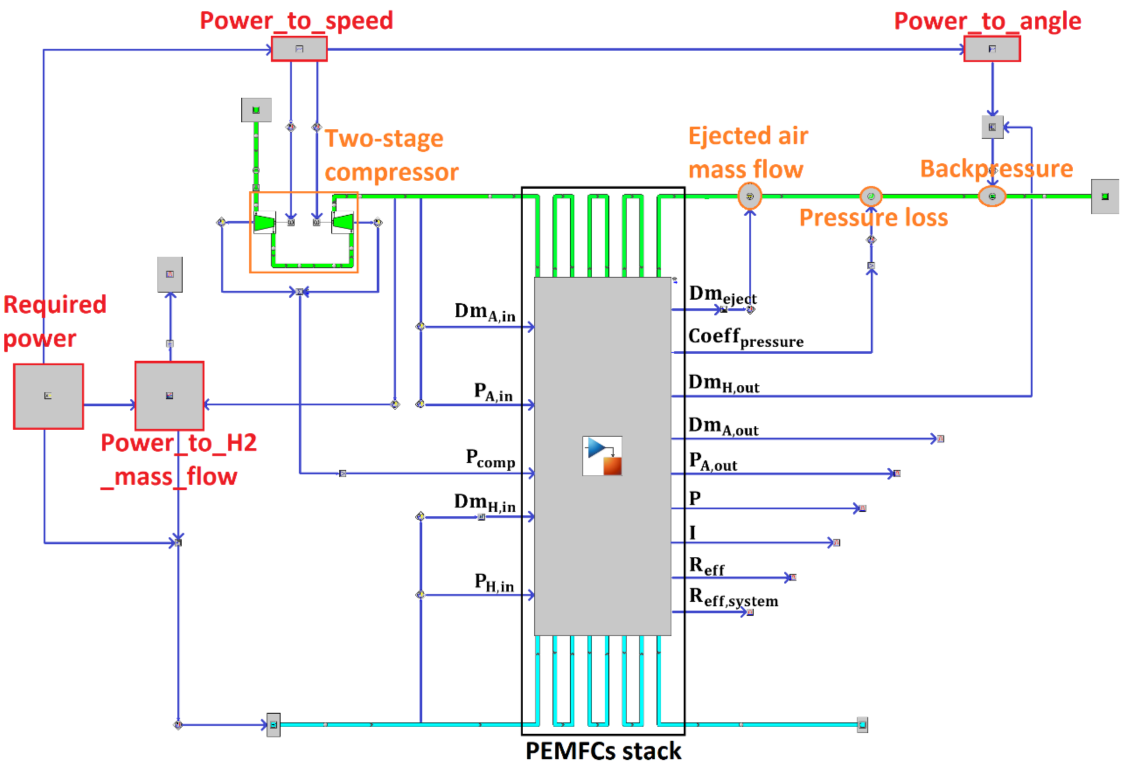

Fig. 2: GT-SUITE diagram of a PEMFCs stack model equipped with a two-stage electric compressor

As seen in Fig. 2, the GT-SUITE model takes into consideration the air consumed through the stack. Dm_{eject} is the part of air consumed during the electrochemical reaction. It is used to model the decrease of air mass flow rate through the stack due to the oxygen consumption. $Coeff_{pressure}$, which is calculated with an equation from GT-SUITE, is used to take into consideration the pressure loss through the stack due to oxygen consumption. The GT-SUITE equation is a simplified model of pressure loss. So, a gain has been added to consider the compressible character of the air.

5- Results

The automatic control of different parameters (backpressure, hydrogen mass flow, compressor speed and so on) allows to proceed to a simulation of the Worldwide Harmonised Light Vehicle Test Procedure (WLTP) driving cycle. As seen in Fig. 3, this 23.3 kilometres driving cycle includes realistic urban and extra-urban driving conditions with credible acceleration and deceleration times.

To compare air supply systems, two different PEMFC stacks have been considered. Both of them have a 350 cm^2 active area and reach a 78 kW maximum output power. The first one is a 360 cells stack equipped with the E-turbocharger or a single stage compressor. The second one is a 315 cells stack equipped with the two-stage compressor. As a result, vehicles equipped with the 315 cells stack weights 1850 kg whereas 360 cells stack vehicles have a 5 kg excess weight [24].

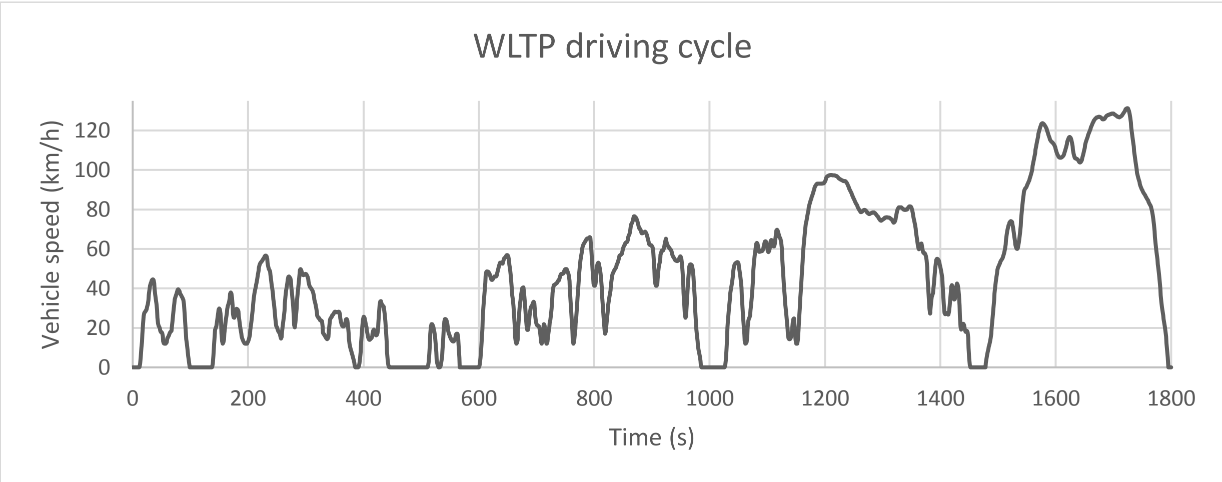

Fig. 3: Vehicle speed through the WLTP driving cycle

The stack provides the entire power to propel the car and to drive the air supply system. In each case, the air supply system has been optimized to reach the highest system electric efficiency and so the highest driving range with a 5.6 kg of hydrogen storage tank [25]. Both of stacks operate with a constant 3 bars pressure for the hydrogen supply system and operate at 80°C.

Table 3: partial results of WLTP driving cycle simulation

Configuration number	**1**	**2**	**3**
Number of cells	360		315
Air supply system	E-turbocharger	Single stage compressor	Two-stage compressor
Pressure range (bar)	[1.1 – 2.3]	[1.1 – 2.2]	[1.1 – 2.7]
Average system electric efficiency (%)	32.1	28.8	30.5
Average stack electric efficiency (%)	61.7	61.6	61.2
Average compressor/ turbine efficiency (%)	76.8 / 51.6	77.9 / –	60.2 / –
Driving range (km) for 5.6 kg of hydrogen	706	682	681

The same compressor has been used for configuration 1 and 2. Only the rotation power map has been adapted for each configuration. The single stage compressor uses a backpressure whereas the E-turbocharger has a turbine at the stack outlet. As seen in table 3, the E-turbocharger system reaches a higher system electric efficiency average and so a 3.5 % higher driving range. Thanks to the turbine, the average power to provide to the E-turbocharger is 46% lower than the required average power for the single stage compressor (mainly attributable to low speed period). During the maximum acceleration phase, the turbine reaches to recover 2.4 kW and so 20% of power required relative difference.

By reducing the number of cells, the mass transfer losses increase since it is harder for reactants to reach the catalysis area. As seen in Fig. 4, the stack electric efficiency decreases. The two-stage compressor has been designed to reach 4.0 bar. During the WLTP driving cycle, the two-stage compressor average pressure is 4.9% higher than the E-turbocharger one which could have compensated the increase of mass transfer losses. However, the two-stage compressor average power required is 43% higher than the power required by the E-turbocharger. This leads to a 1.6% absolute change lower system electric efficiency average and a 3.5% lower driving range than the E-turbocharger configuration.

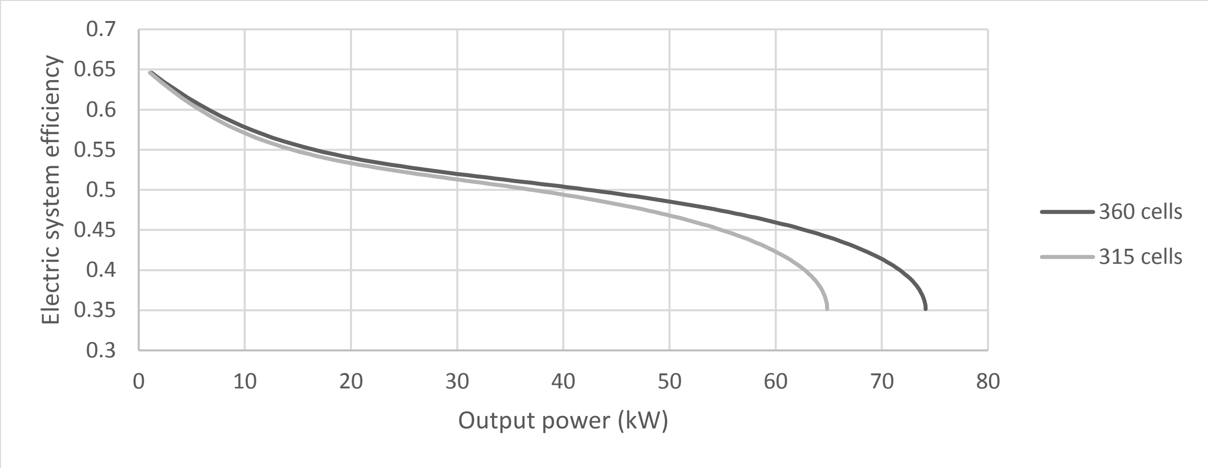

Fig. 4: impact of the number of cells on the stack electric efficiency (operating at 2 bar)

Conclusion

Simulations have shown that a vehicle equipped with E-turbocharger have higher stack performances (relative variation from 5.2% to 11.5% regarding the electric system efficiency average) and driving range (increasing from 3.5% to 3.7% regarding the driving range) than the others. This result aligns with the current FCV manufacturers' trend to use E-turbocharger. However, the compactness gain obtained by using a two-stage compressor cannot be ignored. If the driving range is targeted, the E-turbocharger is the most suitable choice. However, for a low centre of gravity and a better handling, the two-stage compressor is a better choice than an E-turbocharger. To confirm this result, it could be interesting to check the validity of the fuel cell model used and to compare the difference in weight between an E-turbocharger and a two-stage compressor in order to obtain more accurate driving range forecast.

References:

1. Edenhofer, O., R. Pichs-Madruga, Y. Sokona, E. Farahani et al. Climate change 2014: mitigation of climate change. Contribution to the Fifth Assessment Report of the Intergovernmental Panel on Climate Change Cambridge University Press, 2014

2. The Union of Concerned Scientists. How clean are hydrogen fuel cell electric vehicles? , September 2014

3. Mahmoudzadeh Andwari, A., Pesiridis, A., Rajoo, S., Martinez-Botas, R. and Esfahanian, V., "A Review of Battery Electric Vehicle Technology and Readiness Levels", Renewable and Sustainable Energy Reviews, Volume 78, October 2017, Pages 414–430. https://doi.org/10.1016/j.rser.2017.03.138

4. Tsuyoshi Maruo, Masashi Toida, Tomohiro Ogawa, Yuji Ishikawa, Hiroyuki Imanishi et al. Development of motorized turbo compressor for Clarity Fuel Cell, SAE international, March 2017, 2017-01-1187

5. Office of Energy Efficiency and Renewable Energy. Types of fuel cells [accessed: 25 April 2018] https://www.energy.gov/eere/fuelcells/types-fuel-cells

6. Fuelcell.co.uk, 2010 [accessed: 23 April 2018] http://www.fuelcell.co.uk/proton-exchange-membrane-fuel-cells/

7. Ulf Bossel. Rapid startup SOFC modules, Fuel Cells 2012 Science & Technology – A Grove Fuel Cell Event, Energy Procedia, Volume 28, 2012, Pages 48 – 56. https://doi.org/10.1016/j.egypro.2012.08.039

8. Nissan GB. Nissan unveils world's first solid-oxide fuel cell vehicle, Nissan newsroom, August 2016 [accessed: 15 May 2018] https://newsroom.nissan-europe.com/uk/en-gb/media/pressreleases/148584/nissan-unveils-worlds-first-solid-oxide-fuel-cell-vehicle1

9. Steve Barrett, Toyota begins sales of Sora fuel cell bus, Fuel Cells Bulletin, Volume 2018, April 2018 [accessed: 5 June 2018]

10. S.P.S. Badwal, S. Giddey, A. Kulkarni, J. Goel, S. Basu. Direct ethanol fuel cells for transport and stationary applications – a comprehensive review, Applied Energy 145, 2015, Pages 80–103. https://doi.org/10.1016/j.apenergy.2015.02.002

11. Yu, W., Sichuan, X., and Ni, H., "Air Compressors for Fuel Cell Vehicles: An Systematic Review", SAE Int. J. Alt. Power. 4(1):2015, doi:10.4271/2015-01-1172

12. Walters, M., Wick, M., Pischinger, S., Ogrzewalla, J. et al., "Fuel Cell System Development: A Strong Influence on FCEV Performance," SAE Technical Paper 2018-01-1305, 2018, doi:10.4271/2018-01-1305

13. Hasegawa, T., Imanishi, H., Nada, M., and Ikogi, Y., "Development of the Fuel Cell System in the Mirai FCV", SAE Technical Paper 2016-01-1185, 2016, doi:10.4271/2016-01-1185

14. Martinez-Botas, R., Pesiridis, A. and Yang, M., "Overview of Boosting Options for Future Downsized Engines", Science China Technological Sciences Journal, Vol. 54, No.2, February 2011, doi: 10.1007/s11431-010-4272-1.

15. Feneley, A., Pesiridis, A. and Mahmoudzadeh Andwari, A "Variable Geometry Turbocharger Technologies for Exhaust Energy Recovery and Boosting - A Review", Renewable and Sustainable Energy Reviews, Volume 71, Pages 959 – 975, 2017. http://dx.doi.org/10.1016/j.rser.2016.12.125

16. T Fischer, OW Willers, JR Seume. Preliminary design of a partial admission turbine for waste heat recovery in fuel cells, 13th International Conference on Turbochargers and Turbocharging Conference Proceedings, London, UK, May 2018, ISBN: 978-0-9956263-3-1

17. Pukrushpan J.T, Stefanopoulou A.G, Peng H. Control of fuel cell power systems: principles, modeling, analysis and feedback design, Springer Science & Business Media: Berlin, Germany, 2004, ISBN: 1-85233-816-4

18. Alan Cruz Rojas, Guadalupe Lopez Lopez, J. F. Gomez-Aguilar, Victor M. Alvarado, Cinda Luz Sandoval Torres. Control of the air supply subsystem in a PEMFC with balance of plant simulation, MDPI, January 2017, doi:10.3390/su9010073

19. Alexander Kabza Fuel cell formulary, November 2016 [accessed: 21 May 2018]

20. Denis Candusso. Hybridation du groupe électrogène à pile à combustible pour l'alimentation d'un véhicule électrique. Energie électrique. Institut National Polytechnique de Grenoble - INPG, 2002, tel-00805698

21. Aeristech Electric superchargers (eSuperchargers), 2015 [accessed: 19 April 2018] http://www.aeristech.co.uk/electric-supercharger/

22. Benedikt Ernst, Jasper Kammeyer, Joerg R. Seume. Improved map scaling methods for small turbocharger compressors, Proceedings of ASME Turbo Expo, 2011, GT2011-45345

23. Clay Bell, Daniel Zimmerle, Thomas Bradley, Daniel Olsen, Peter Young. Scalable turbocharger performance maps for dynamic state-based engine models, International Journal of Engine Research, 2016, Vol. 17(7) 705–712, doi:10.1177/1468087415609855

24. Itoga, M., Hamada, S., Mizuno, S., Nishiumi, H. et al., "Development of Fuel Cell Stack for New FCV", SAE Technical Paper 2016-01-0529, 2016, doi:10.4271/2016-01-0529.

25. Johnson, K., Veenstra, M., Gotthold, D., Simmons, K. et al., "Advancements and Opportunities for On-Board 700 Bar Compressed Hydrogen Tanks in the Progression Towards the Commercialization of Fuel Cell Vehicles", SAE Int. J. Alt. Power. 6(2):2017, doi:10.4271/2017-01-1183.